

12056
Ilmenite Basalt
121 grams

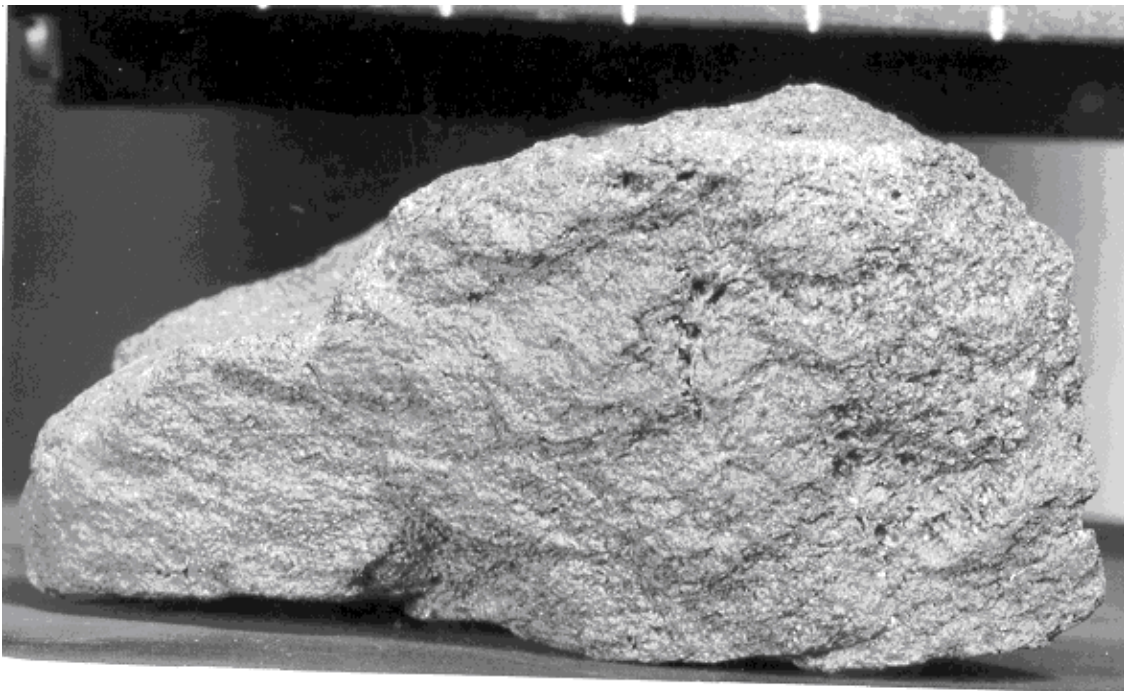


Figure 1: Photo of side of 12056. Scale at top is in cm. NASA #S69-61044.

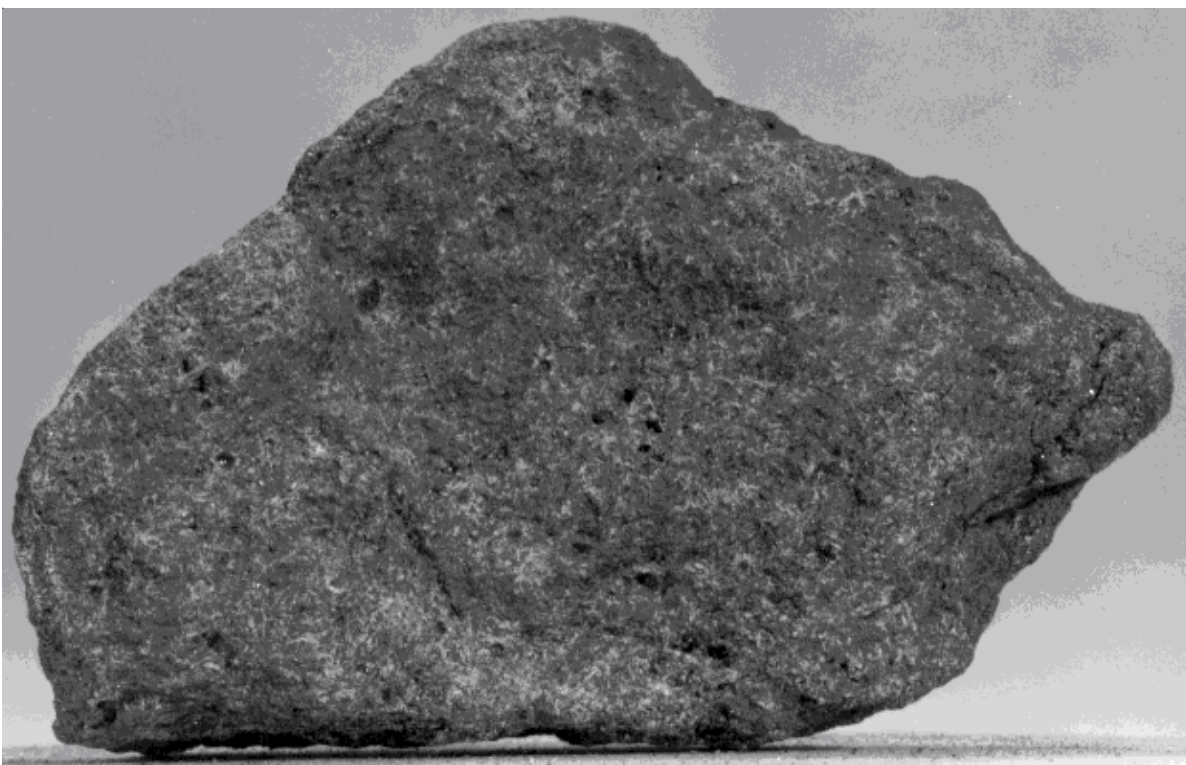


Figure 2: Photo of rounded top of 12056 showing zap pits. Rock is about 7 cm across. NASA # S70-19062.

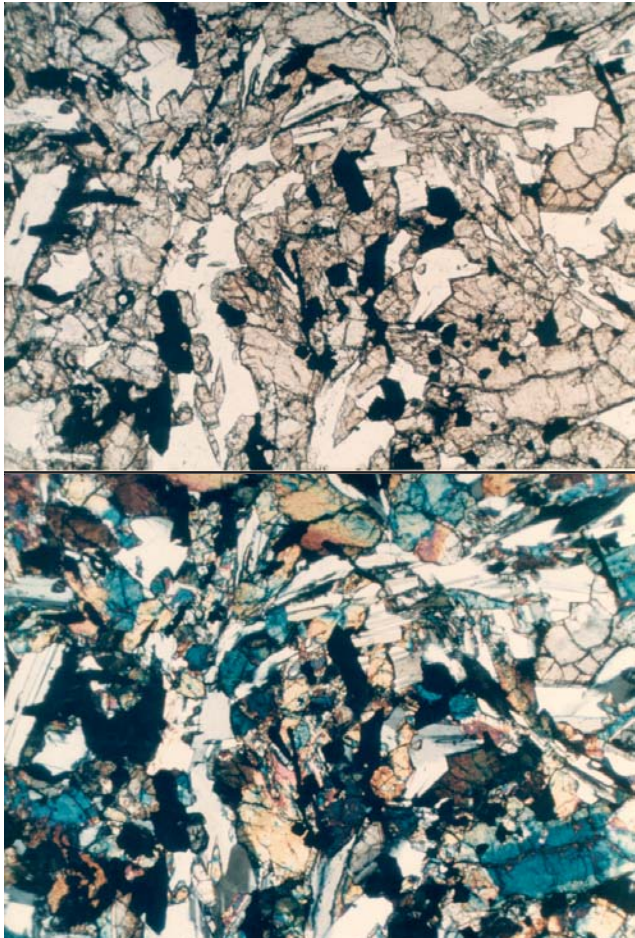


Figure 3: Photomicrograph of thin section 12056.4. Field of view 2.6 mm. NASA S70-49262-263.

Introduction

12056 is a relatively coarse-grained, subophitic basalt dated at 3.2 b.y. The rounded side has micrometeorite craters, while the flat side has none (figure 1 and 2). Neal et al. (1994) classify 12056 as an ilmenite basalt.

Petrography

Dungan and Brown (1977) describe 12056 as “a medium-grained microgabbro with a seriate subophitic texture. The crystallization sequence is olivine, metal, chromian spinel, followed by pyroxene in a peritectic reaction-relationship with olivine, ulvöspinel, plagioclase, ilmenite and mesostasis consisting of silica phase, Si + K-rich glass, fayalite, phosphate, metal and troilite”.

The texture is equigranular to subophitic with grain size about 0.5 mm for olivine, pyroxene, plagioclase and ilmenite (figure 3). The late-stage mesostasis of 12056 consists of several percent symplectoid segregations of fayalite, alkali-rich glass, phosphate,

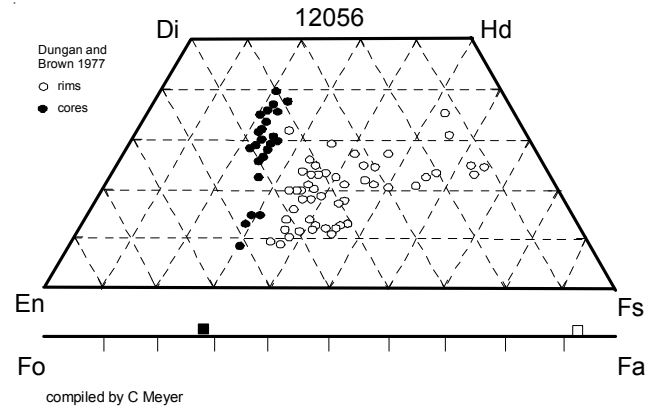


Figure 4: Pyroxene composition for 12056 (adapted from Dungan and Brown 1977).

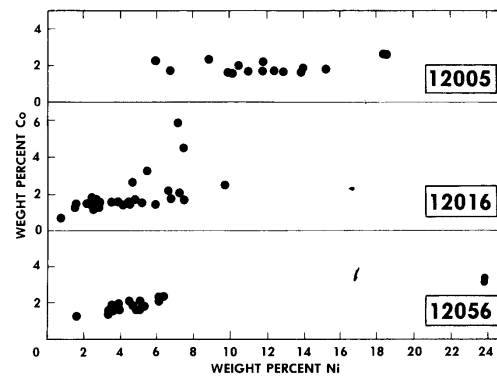


Figure 5: Ni and Co contents of metallic iron grains in 12056 (from Dungan and Brown 1977).

ferroaugite, ilmenite, metal and troilite. The alkali-rich rich glass is an apparent immiscible liquid.

Neal et al. (1994) found that the mode was just like the one reported by Dungan and Brown (1977).

Mineralogy

Olivine: Two kinds of olivine are found in 12056. Partially resorbed olivine cores to pyroxene are as

Mineralogical Mode for 12056

| | Neal et al. 1994 | Dungan and Brown 1977 |
|---------------|---------------------|--------------------------|
| Olivine | 10.8 | 10.8 |
| Pyroxene | 49.2 | 49.2 |
| Plagioclase | 28.8 | 28.8 |
| Ilmenite | 6.8 | 6.8 |
| Chromite +Usp | 1.6 | 1.6 |
| Mesostasis | 2.5 | 2.5 |
| “silica” | 0.8 | 0.8 |

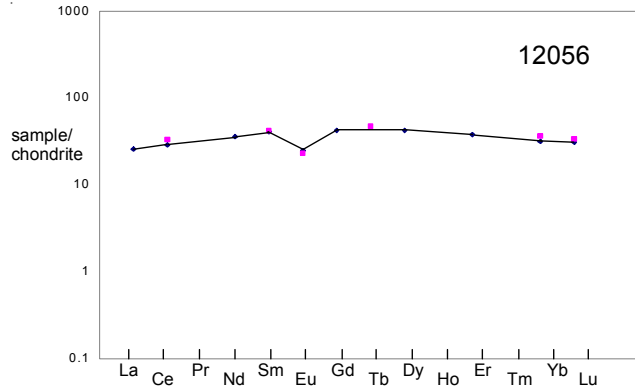


Figure 6: Normalized rare-earth-element content of 12056 (data from Nyquist et al. 1979 connected).

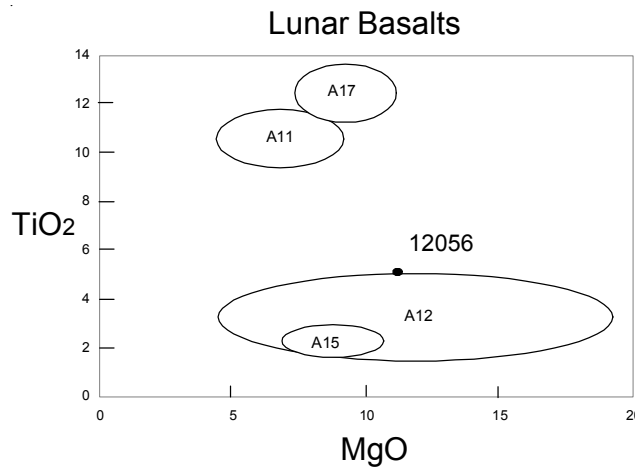


Figure 7: Composition of 12056 compared with that of other lunar basalts.

magnesian as Fo_{72} , while late-stage olivine in the symplectitic intergrowths in mesostasis is Fo_8 (fayalite).

Pyroxene: The cores of large pyroxene grains are dominated by augite although small amounts of low-Ca pyroxene are present (Dungan and Brown 1977). Pyroxene zoning is complex (figure 4) with ferroaugite in the mesostasis.

Plagioclase: Plagioclase is relatively uniform in composition at An_{88} , although the Or content increases near the mesostasis.

Ilmenite: The MgO content of ilmenite is 0.5 to 1.5 %.

Spinel: Cr-rich spinel zones to ulvöspinel (Dungan and Brown 1977).

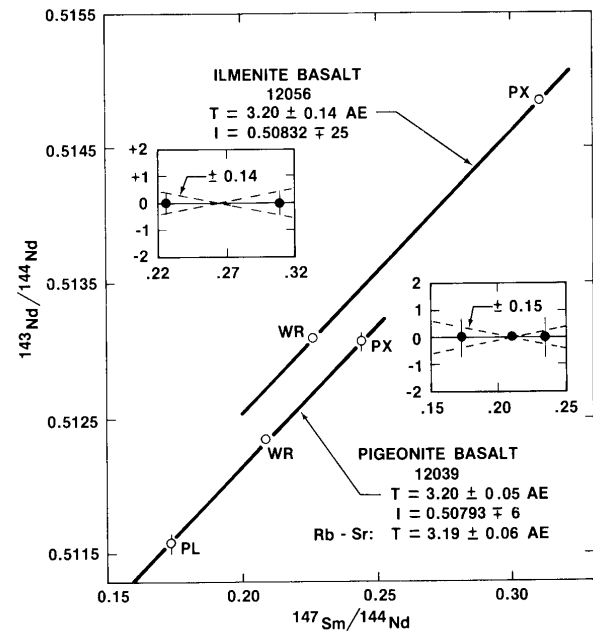


Figure 8: Sm-Nd mineral isochron diagrams for 12039 and 12056 (Nyquist et al. 1979).

Metal: Ni and Co contents in metal grains are high (figure 5).

Chemistry

Rhodes et al. (1977) determined major element composition and Nyquist et al. (1979) determined the rare earth element content (table 1, figure 6).

Radiogenic age dating

Nyquist et al. (1979) determined the age of 12056 by Sm-Nd internal mineral isochron as 3.2 ± 0.14 by (figure 8).

Summary of Age Data for 12056

| | Ar/Ar | Rb/Sr | Nd/Sm |
|---------------------|-------|-------|----------------|
| Nyquist et al. 1979 | | | 3.2 ± 0.14 |

Table 1. Chemical composition of 12056.

| reference weight | Rhodes 77 | Nyquist79 |
|--------------------------------|-----------------------------|----------------|
| SiO ₂ % | 43.44 | (c) |
| TiO ₂ | 5.07 | (c) |
| Al ₂ O ₃ | 8.82 | (c) |
| FeO | 21.6 | (c) |
| MnO | 0.29 | (c) |
| MgO | 9.3 | (c) |
| CaO | 10.21 | (c) |
| Na ₂ O | 0.29 | (a) |
| K ₂ O | 0.07 | (c) 0.066 (b) |
| P ₂ O ₅ | 0.07 | (c) |
| S % | 0.1 | (c) |
| <i>sum</i> | | |
| Sc ppm | 60 | (a) |
| V | | |
| Cr | 3310 | (a) |
| Co | 42 | (a) |
| Ni | | |
| Cu | | |
| Zn | | |
| Ga | | |
| Ge ppb | | |
| As | | |
| Se | | |
| Rb | | 0.785 (b) |
| Sr | 159 | (c) 162 (b) |
| Y | 55 | (c) |
| Zr | 135 | (c) |
| Nb | 6.1 | (c) |
| Mo | | |
| Ru | | |
| Rh | | |
| Pd ppb | | |
| Ag ppb | | |
| Cd ppb | | |
| In ppb | | |
| Sn ppb | | |
| Sb ppb | | |
| Te ppb | | |
| Cs ppm | | |
| Ba | 62 | (b) 58.7 (b) |
| La | | 6.02 (b) |
| Ce | 20.2 | (a) 17.7 (b) |
| Pr | | |
| Nd | | 16.1 (b) |
| Sm | 6.4 | (a) 6.04 (b) |
| Eu | 1.31 | (a) 1.41 (b) |
| Gd | | 8.4 (b) |
| Tb | 1.73 | (a) 10.4 (b) |
| Dy | | |
| Ho | | |
| Er | | 6.12 (b) |
| Tm | | |
| Yb | 6 | (a) 5.29 (b) |
| Lu | 0.82 | (a) 0.745 (b) |
| Hf | 4.8 | (a) |
| Ta | | |
| W ppb | | |
| Re ppb | | |
| Os ppb | | |
| Ir ppb | | |
| Pt ppb | | |
| Au ppb | | |
| Th ppm | | |
| U ppm | | |
| <i>technique</i> | (a) INAA, (b) IDMS, (c) XRF | |

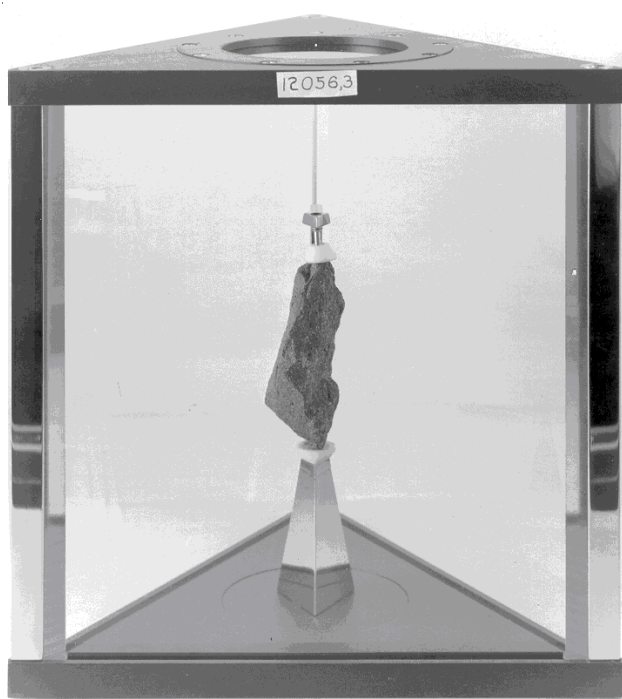
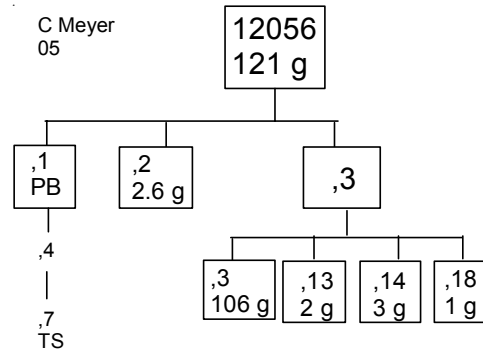


Figure 9: 12056,3 on display.



Processing

Sample 12056,3 has been used for public display (figure 9). There are 7 thin sections.

List of Photo #s for 12056

| | |
|-------------------|---------|
| S69-61051 – 61058 | B & W |
| S69-63839 – 63842 | color |
| S70-19051 – 19062 | B & W |
| S70-22500 – 22511 | |
| S70-17293 – 17294 | display |
| S70-17974 – 17977 | TS |
| S70-49262 – 49263 | TS |
| S70-49841 – 49842 | TS |
| S70-49823 – 49824 | TS |
| S94-035799 | ,3 |

References for 12056

Dungan M.A. and Brown R.W. (1977) The petrology of the Apollo 12 basalt suite. *Proc. 8th Lunar Sci. Conf.* 1339-1381.

James O.B. and Wright T.L. (1972) Apollo 11 and 12 mare basalts and gabbros: Classification, compositional variations and possible petrogenetic relations. *Geol. Soc. Am. Bull.* **83**, 2357-2382.

LSPET (1970) Preliminary examination of lunar samples from Apollo 12. *Science* **167**, 1325-1339.

Neal C.R., Hacker M.D., Snyder G.A., Taylor L.A., Liu Y.-G and Schmitt R.A. (1994a) Basalt generation at the Apollo 12 site, Part 1: New data, classification and re-evaluation. *Meteoritics* **29**, 334-348.

Neal C.R., Hacker M.D., Snyder G.A., Taylor L.A., Liu Y.-G and Schmitt R.A. (1994b) Basalt generation at the Apollo 12 site, Part 2: Source heterogeneity, multiple melts and crustal contamination. *Meteoritics* **29**, 349-361.

Nyquist L.E., Bansal B.M., Wooden J. and Wiesmann H. (1977) Sr-isotopic constraints on the petrogenesis of Apollo 12 mare basalts. *Proc. 8th Lunar Sci. Conf.* 1383-1415.

Nyquist L.E., Shih C.-Y., Wooden J.L., Bansal B.M. and Wiesmann H. (1979) The Sr and Nd isotopic record of Apollo 12 basalts: Implications for lunar geochemical evolution. *Proc. 10th Lunar Planet. Sci. Conf.* 77-114.

Papike J.J., Hodges F.N., Bence A.E., Cameron M. and Rhodes J.M. (1976) Mare basalts: Crystal chemistry, mineralogy and petrology. *Rev. Geophys. Space Phys.* **14**, 475-540.

Rhodes J.M., Blanchard D.P., Dungan M.A., Brannon J.C., and Rodgers K.V. (1977) Chemistry of Apollo 12 mare basalts: Magma types and fractionation processes. *Proc. 8th Lunar Sci. Conf.* 1305-1338.